Supporting Information

Activation of Sodium Storage Sites in Prussian Blue Analogues via Surface Etching

Wenhao Ren,[†] *Mingsheng Qin,*[†] *Zixuan Zhu,*[†] *Mengyu Yan,*[‡] *Qi Li,**[†] *Lei Zhang,*[†] *Dongna Liu,*[†] *and Liqiang Mai**[,†,§]

[†]State Key Laboratory of Advanced Technology for Materials Synthesis and Processing, Wuhan University of Technology, Wuhan 430070, China

[§]Department of Chemistry, University of California, Berkeley, California 94720, United States

[‡] Materials Science and Engineering Department, University of Washington, Seattle, Washington 98195-2120, United States

Corresponding Author

* E-mail: mlq518@whut.edu.cn

* E-mail: qi.li@whut.edu.cn

Experimental Section

Synthesis of PBAs nanocubes and etching procedure: $Na_4Fe(CN)_6 \cdot 10H_2O$, $NiCl_2 \cdot 6H_2O$, NaOH and $Na_3C_6H_5O_7$ were analytical grade and purchased from the Sinopharm Chemical Reagent Co., Ltd. (Shanghai, China). First, $Na_4Fe(CN)_6 \cdot 10H_2O$ (5 mmol) was added in 250 ml water with stirring for 5 min to obtain the clear solution A. $Na_3C_6H_5O_7$ (20 mmol) and $NiCl_2 \cdot 6H_2O$ (1 g) were added in another 250 ml water with stirring for 5 min to obtain the clear solution B. The solution A was poured into solution B under magnetic stirring for 10 min. Then, the mixture was aged at room temperature for 48 h to get the precipitate. After that, The as-obtained $Na_xNiFe(CN)_6$ nanocubes were filtered, washed with deionized water and dried overnight in vacuum oven at 80 °C. In the end, the prepared $Na_xNiFe(CN)_6$ nanocubes (100 mg) and $Na_3C_6H_5O_7$ (5 mmol) were dispersed in 0.4 M NaOH solution by sonication for 6 h. The products were collected by centrifugation, and washed with water and ethanol for several times. Finally, the samples were dried at 80 °C in vacuum for 24 h.

Characterization: XRD measurement was performed to investigate the crystallographic information using a D8 Advance X-ray diffractometer with Co Kα X-ray source. Field emission scanning electron microscopy (FESEM) images was collected with a JEOL JSM-7100F at an acceleration voltage of 10 kV. Fourier transformed infrared (FTIR) transmittance spectra were recorded using a 60-SXB IR spectrometer. Raman spectra were obtained using a Renishaw INVIA micro-Raman spectroscopy system. BET surface areas were measured using Tristar II 3020 instrument by nitrogen adsorption of at 77 K. Inductively coupled plasma (ICP) tests were carried out using an Optima 4300DV. XPS measurements were performed using a VG MultiLab 2000 instrument.

Electrochemical Measurements: The electrochemical measurements were tested with 2016 coin cells assembled in a glove box filled with pure argon gas. For sodium battery, sodium foil was used as the anode, a 1 M solution of $NaClO_4$ in ethylene carbon (EC)–dimethyl carbonate (DMC) (1 : 1 w/w) and 5% FEC was used as the electrolyte, and a Whatman Glass Microfibre Filter (Grade GF/F) was used as the separator. For lithium battery, lithium foil was used as the anode and 1 M solution of

LiPF6 in ethylene carbon (EC)/dimethyl carbonate (DMC) was used as the electrolyte. The cathode electrode was produced with 60 wt% active material, 30 wt% ketjen black and 10 wt% poly(tetrauoroethylene) (PTFE). The mass loading of the active material was 2-3 mg cm^{-2}. The battery was aged for 12 h before test to ensure full absorption of the electrolyte into the electrodes. Galvanostatic charge/discharge measurements were performed with a multichannel battery testing system (LAND CT2001A). CV and EIS were performed with an electrochemical workstation (Autolab PGSTAT302N).

Calculation of Na^+ diffusion coefficients through GITT results[1]*:* The D^{GITT} can be obtained from the potential response to a small constant current pulse (10 mA g^{-1}) via the following Eq. (1):

$$\boldsymbol{D^{GITT} = \frac{4}{\pi\tau}\left(\frac{m_B V_M}{M_B S}\right)^2\left(\frac{\Delta E_S}{\Delta E_\tau}\right)^2} \quad (1)$$

Where τ is the constant current pulse time, m_B, V_M, S, and M_B are the mass, molar volume, electrode–electrolyte interface area, and molar mass of NiHCF, respectively. In Figure S6, ΔE_S is the voltage difference during the open circuit period, and ΔE_τ is the total change of cell voltage during a constant current pulse excluding the *IR* drop.

Calculation of Na^+ apparent diffusion coefficients through EIS results[2]*:* The diffusion coefficient value (D^{EIS}) can be calculated from the Eq. (2) and Eq. (3):

$$Z' = R_e + R_{ct} + \sigma_w \omega^{-1/2} \quad (2)$$

$$D = 0.5(RT/An^2F^2\sigma_w C)^2 \quad (3)$$

In eqn (2), ω ($2\pi f$) is the angular frequency in the low frequency region, and both R_e and R_{ct} are kinetics parameters independent of frequency. Then, the Warburg coefficient (σ_w) can be obtained from the slope of the fitting line (Figure S7). In eqn (3), R is the gas constant, T is the temperature, A is the area of the electrode, n is the number of electrons transfer per mole of the active material involved in the electrode reaction, F is Faraday's constant and C is the molar concentration of Na ions.

Calculation of Na^+ apparent diffusion coefficients through CV results[3,4]*:* The diffusion coefficient value (D^{CV}) can be calculated from the Eq. (4):

$$I_p = 2.69 \times 10^5 \, n^{3/2} A D^{1/2} \, Cv^{1/2} \quad (4)$$

where I_p is the peak current (A), n is the number of electrons per molecule during the intercalation, A is the surface area of the cathode (cm^2), C is the concentration of Na ions in the electrode (mol cm^{-3}), and v is the scanning rate (V s^{-1}).

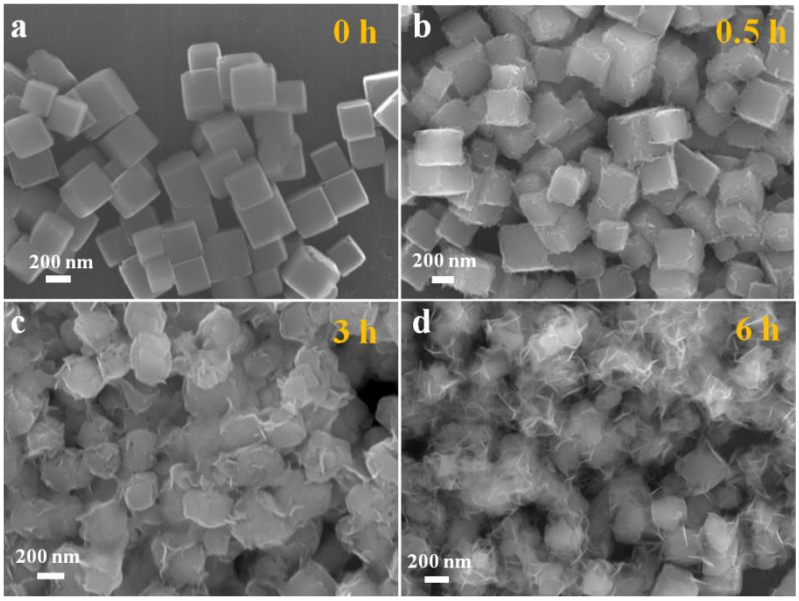

Figure S1. FESEM images of the etching products after reaction time for (a) 0 h, (b) 0.5 h, (c) 3 h, (d) 6 h.

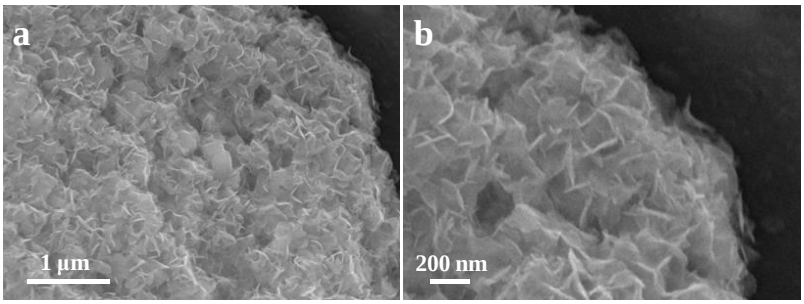

Figure S2. (a) Low-resolution and (b) high-resolution SEM images of the NiHCF products after the etching time of 10 h.

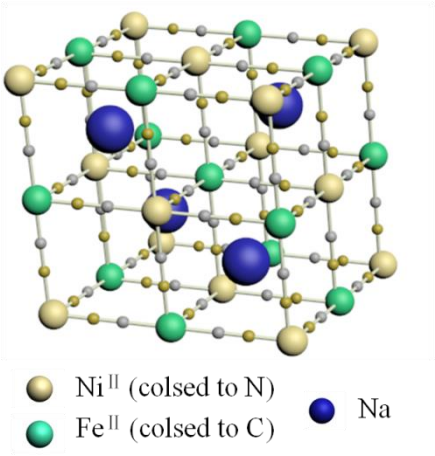

Figure S3. The crystal structure of rhombohedral NiHCF.

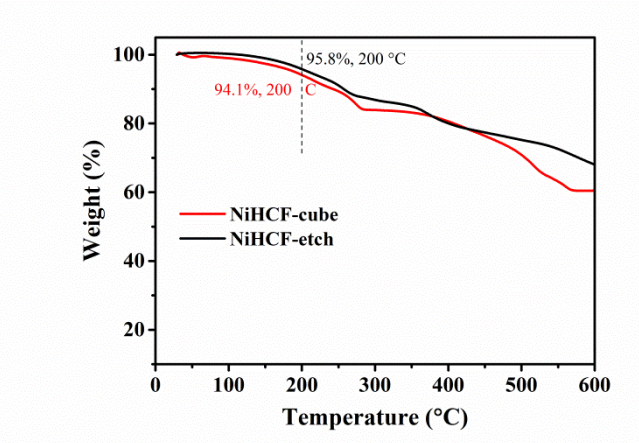

Figure S4. TG curves of NiHCF-cube and NiHCF-etch.

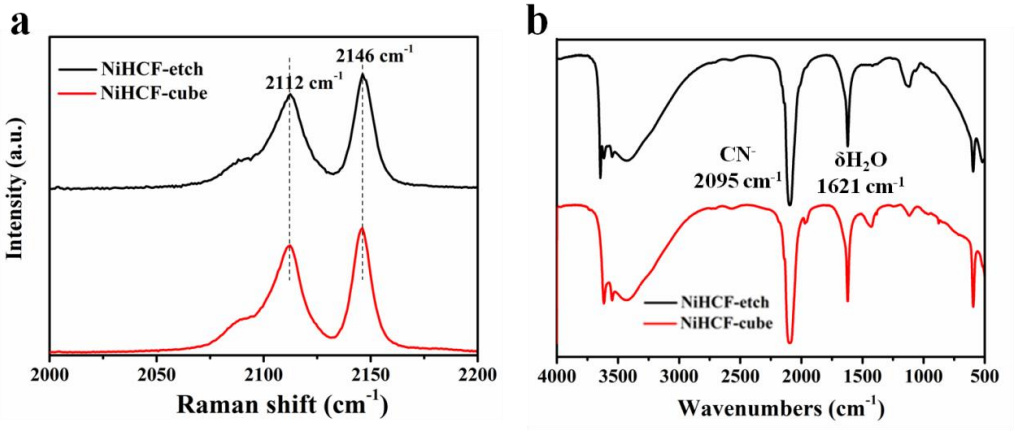

Figure S5. (a) Raman spectra of the NiHCF-cube and NiHCF-etch. The two peaks located at 2112 cm^{-1} and 2146 cm^{-1} in Raman spectra are corresponding to the vibrations of CN group in Fe^{II}-CN-Ni^{II}, and no Fe^{III}-CN-Ni^{II} peak is observed.[5] (b) FT-IR spectra of NiHCF-cube and NiHCF-etch. FT-IR profiles also confirm that the bonding state of NiHCF-etch remains unchanged after the etching process.[6]

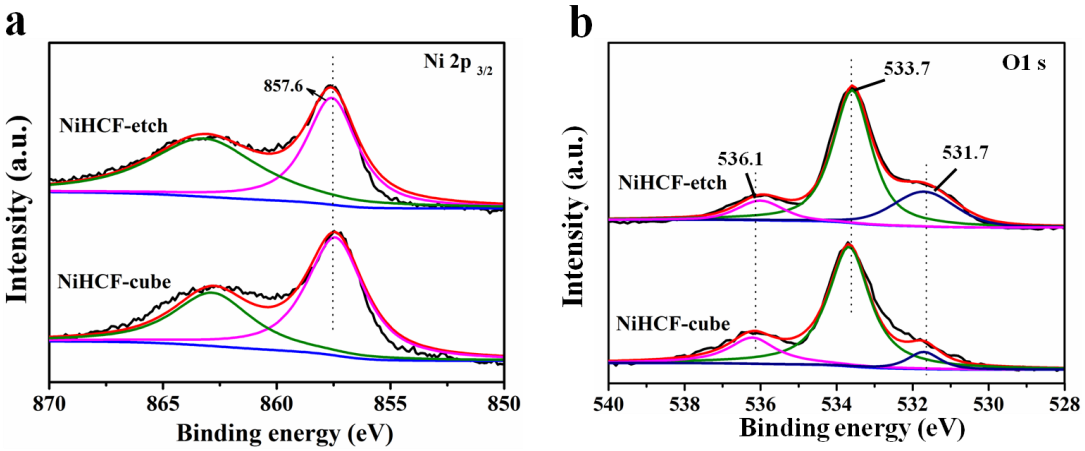

Figure S6. XPS spectra of the (a) NiHCF-cube and (b) NiHCF-etch. The peaks located at 536.2 eV and 533.7 eV remain unchanged during the etching process, which correspond to the physic/chemi-sorbed water and the oxygen ions in low coordination at the surface, respectively. Besides, the intensity of the peak at 531.7 eV becomes stronger after etching. This peak is usually associated with oxygen in OH^- groups and the increase of this contribution in the O 1s spectrum indicates that the surface of the NiHCF-etch is slightly hydroxylated as a result of the substitution of oxygen atoms or vacancies at the surface by hydroxyl groups.[7]

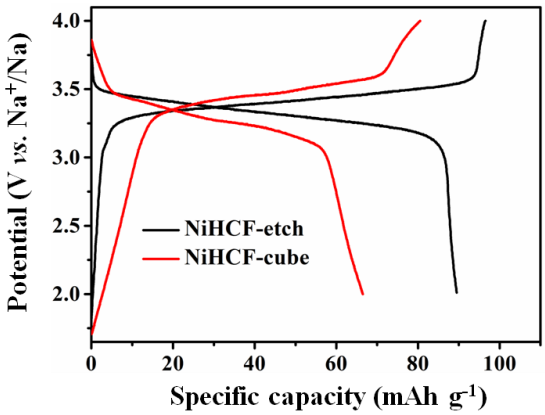

Figure S7. The charge-discharge curves of NiHCF-etch and NiHCF-cube at the first cycle with a current of 1.1 C.

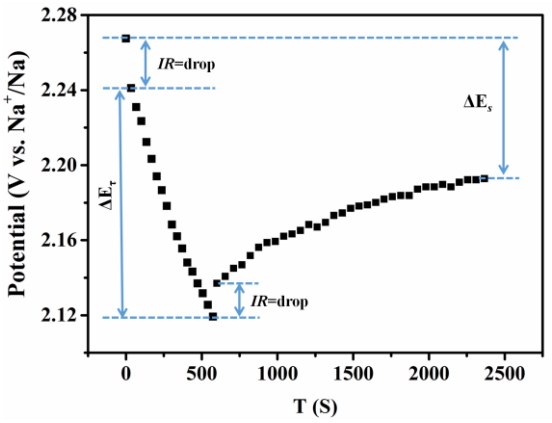

Figure S8. GITT potential response curve with time.

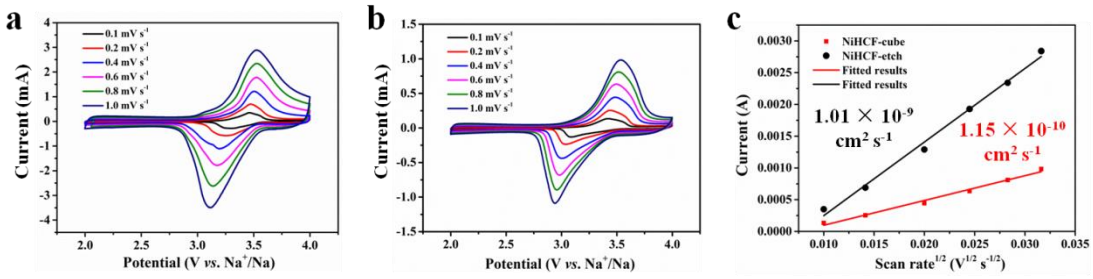

Figure S9. The CV curves of (a) NiHCF-etch and (b) NiHCF-cube at different scan rate from 0.1 to 1.0 mV s^{-1}. (c) The relation between the square root of the scan rate ($v^{1/2}$) and the corresponding currents for oxidation peaks. It is found that the peak currents for both electrodes display a linear relation with the square root of the scan rate ($v^{1/2}$). The calculated D^{CV} of NiHCF-etch is about an order of magnitude higher than NiHCF-cube, conforming to the GITT and EIS results.

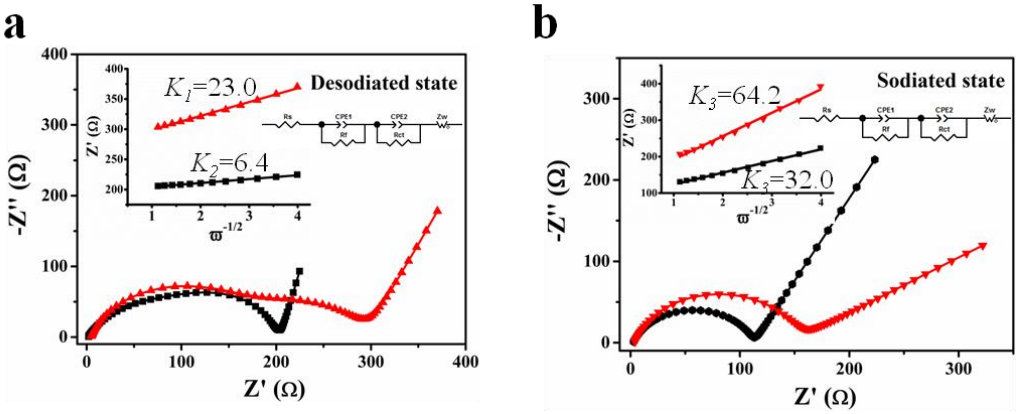

Figure S10. EIS results of (a) desodiated and (b) sodiated state of NiHCF-cube (red curves) and NiHCF-etch (black curves), inset is the calculation of Warburg factor σ ($Z_w \propto \sigma\omega^{-1/2}$). In the desodiated state, the charge transfer resistance (R_{ct}) of NiHCF-cube and NiHCF-etch is 129.3 and 65.6 Ω, and their D^{EIS} calculated from Warburg factor (σ) is 3.12×10^{-11} and 4.03×10^{-10} cm^2 s^{-1}, indicating a faster surface reaction kinetics of NiHCF-etch. After sodiation process, the R_{ct} and D^{EIS} of both electrodes exhibit similar degradation trends, and the D^{EIS} of NiHCF-cube and NiHCF-etch decrease to 1.61×10^{-11} and 4.00×10^{-12} cm^2 s^{-1}, which is consistent with GITT analysis.

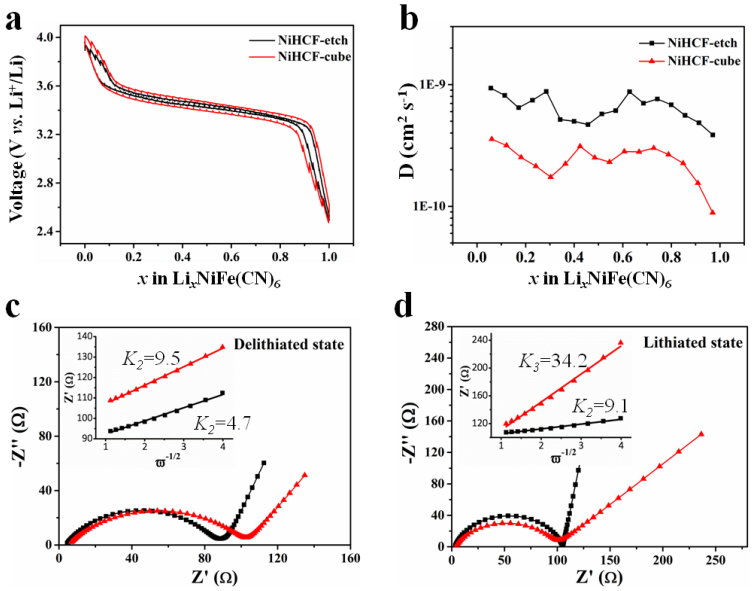

Figure S11. (a) The GITT results of NiHCF-cube and NiHCF-etch *vs*. Li^+/Li. (b) The calculated diffusion coefficients versus state of discharge. EIS results of (c) delithiated and (d) lithiated state of NiHCF-cube (red curves) and NiHCF-etch (black curves), inset is the calculation of Warburg factor σ ($Z_w \propto \sigma\omega^{-1/2}$). It is obvious that the diffusion coefficients of NiHCF-etch *vs*. Li^+/Li are also higher than NiHCF-cube, whcih is consistent with sodiated/desodiated processes.

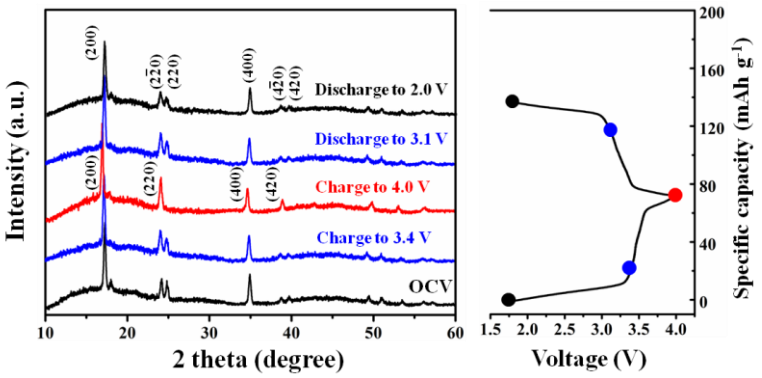

Figure S12. *Ex situ* XRD analysis of NiHCF-cube from 2 V to 4 V.

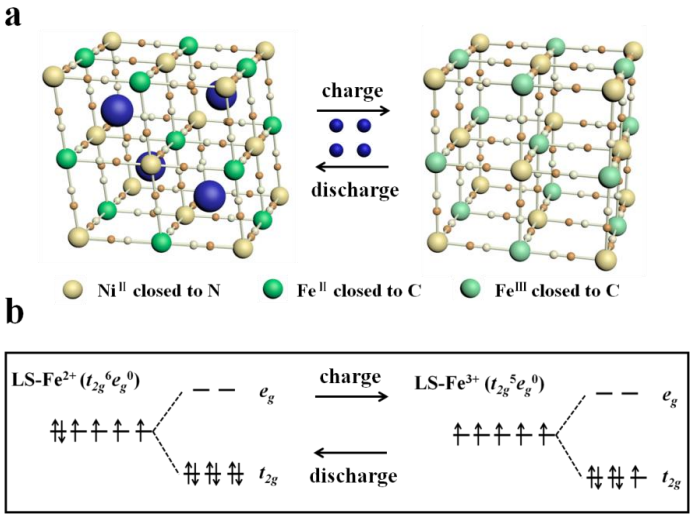

Figure S13. (a) Crystal structure evolution of NiHCF-etch during charge-discharge process. (b) The crystalline field diagram of LS-Fe^{2+} and LS-Fe^{3+} at discharged and charged states.

Table S1. ICP results of the NiHCF-etch and NiHCF-cube.

Number	Element	Weight%	Atomic%
NiHCF-etch	Na	0.66	0.54
	Fe	1.15	0.39
	Ni	1.51	0.49
NiHCF-cube	Na	0.86	0.68
	Fe	2.00	0.65
	Ni	2.28	0.71

Table S2. The sodium storage properties of reported Prussian Blue Analogues.

Cathode	Cycle life (capacity retention)	Rate (capacity retention)	Capacity of Fe^{LS}(C)
Our work	5000 (83.2%)	44.4 C (79%)	90 mAh g^{-1}
$Na_xNiFe(CN)_6$[8]	500 (90%)	1000 mA g^{-1} (60%)	62 mAh g^{-1}
$Na_xNiFe(CN)_6$[9]	/	500 mA g^{-1} (78%)	65 mAh g^{-1}
$Na_xFeFe(CN)_6$/CNT[10]	1000 (81%)	6 C (83%)	70 mAh g^{-1}
$Na_xFeFe(CN)_6$@C[11]	2000 (90%)	90 C (67%)	45 mAh g^{-1}
$Na_xFeFe(CN)_6$[12]	150 (~100%)	600 mA g^{-1} (42%)	40 mAh g^{-1}
$FeFe(CN)_6$[13]	500 (83%)	20 C (82%)	45 mAh g^{-1}
$Na_xMnFe(CN)_6$@ppy[14]	200 (67%)	40 C (42%)	/
$Na_xMnFe(CN)_6$[15]	500 (75%)	20 C (80%)	/

Table S3. The coulombic efficiencies of NiHCF-cube and NiHCF-etch calculated from EIS results.

Sample	Desodiated	Sodiated	Delithiated	Lithiated
NiHCF-etch	4.03×10^{-10}	1.61×10^{-11}	7.47×10^{-10}	1.99×10^{-10}
NiHCF-cube	3.12×10^{-11}	4.00×10^{-12}	1.82×10^{-10}	1.42×10^{-11}

Reference

1. An, Q.; Li, Y.; Yoo, H. D.; Chen, S.; Ru, Q.; Mai, L.; Yao, Y. *Nano Energy* **2015,** *18*, 265-272.
2. Wang, H.; Huang, K.; Ren, Y.; Huang, X.; Liu, S.; Wang, W. *J. Power Sources* **2011,** *196*, 9786-9791.
3. Brezesinski, T.; Wang, J.; Tolbert, S. H.; Dunn, B. *Nat. Mater.* **2010,** *9*, 146.
4. Augustyn, V.; Come, J.; Lowe, M. A.; Kim, J. W.; Taberna, P. L.; Tolbert, S. H.; Abruña, H. D.; Simon, P.; Dunn, B. *Nat. Mater.* **2013,** *12*, 518-522.
5. Jeerage, K. M.; And, W. A. S.; Schwartz, D. T. *Langmuir* **2002,** *18*, 3620-3625.
6. Kulesza, P. J.; Malik, M. A.; And, A. D.; Strojek, J. *Anal. Chem.* **1996,** *68*, 2442-2446.
7. Marco, J. F.; Gancedo, J. R.; Gracia, M.; Gautier, J. L.; Ríos, E.; Berry, F. J. *J. Solid State Chem.* **2000,** *153*, 74-81.
8. Zhang, W.; Zhao, Y.; Malgras, V.; Ji, Q.; Jiang, D.; Qi, R.; Ariga, K.; Yamauchi, Y.; Liu, J.; Jiang, J. S.; Hu, M. *Angew. Chem.* **2016,** *55*, 8228-8234.
9. Yue, Y.; Binder, A. J.; Guo, B.; Zhang, Z.; Qiao, Z. A.; Tian, C.; Dai, S. *Angew. Chem. Inter. Ed.* **2014,** *53*, 3134-3137.

10. You, Y.; Yao, H. R.; Xin, S.; Yin, Y. X.; Zuo, T. T.; Yang, C. P.; Guo, Y. G.; Cui, Y.; Wan, L. J.; Goodenough, J. B. *Adv. Mater.* **2016,** *28*, 7243-7248.
11. Jiang, Y.; Yu, S.; Wang, B.; Li, Y.; Sun, W.; Lu, Y.; Yan, M.; Song, B.; Dou, S. *Adv. Funct. Mater.* **2016,** *26*, 5315-5321.
12. You, Y.; Wu, X. L.; Yin, Y. X.; Guo, Y. G. *Energy Environ. Sci.* **2014,** *7*, 1643-1647.
13. Wu, X.; Luo, Y.; Sun, M.; Qian, J.; Cao, Y.; Ai, X.; Yang, H. *Nano Energy* **2015,** *13*, 117-123.
14. Li, W. J.; Chou, S. L.; Wang, J. Z.; Wang, J. L.; Gu, Q. F.; Liu, H. K.; Dou, S. X. *Nano Energy* **2015,** *13*, 200-207.
15. Song, J.; Wang, L.; Lu, Y.; Liu, J.; Guo, B.; Xiao, P.; Lee, J. J.; Yang, X. Q.; Henkelman, G.; Goodenough, J. B. *J. Am. Chem. Soc.* **2015,** *137*, 2658-2664.